IEEE Access
Multidisciplinary | Rapid Review | Open Access Journal

IEEE VEHICULAR TECHNOLOGY SOCIETY SECTION

Received 28 December 2022, accepted 14 January 2023, date of publication 19 January 2023, date of current version 24 January 2023.

Digital Object Identifier 10.1109/ACCESS.2023.3238056

RESEARCH ARTICLE

Research on the Emergency Obstacle Avoidance Strategy of Intelligent Vehicles Based on a Safety Distance Model

SHENGQIN LI AND QINGQING ZHAO
School of Transportation, Northeast Forestry University, Harbin 150040, China
Corresponding author: Qingqing Zhao (837858480@qq.com)

This work was supported by the Fundamental Research Funds for the Central University in China under Grant 2572019BG01.

ABSTRACT Under emergency conditions, the safety distance between vehicles is insufficient, and drivers initiate unreasonable obstacle avoidance, which results in accident risks to vehicles. Therefore, an emergency obstacle avoidance system is needed for intervention to avoid traffic accidents. This paper proposes a coordinated steering and braking obstacle avoidance control strategy based on a safety distance model. The strategy takes into account handling stability and ride comfort. In the emergency braking obstacle avoidance module, the safety distance model and the graded warning mechanism based on the braking process are established. In the emergency steering obstacle avoidance module, a steering safety distance mode with multiple constraints is established, the obstacle avoidance trajectory is planned using the fifth-degree polynomial, and the obstacle avoidance trajectory is tracked using the model predictive control algorithm. The co-simulation results show that the emergency obstacle avoidance strategy proposed in this paper can select the appropriate way to complete obstacle avoidance under different working conditions. In braking obstacle avoidance, the braking deceleration essentially matches the expected value. In steering obstacle avoidance, the maximum error of lateral displacement can be reduced to 0.09 m. The research in this paper can provide a theoretical and practical basis for improving the driving safety, handling stability and ride comfort of intelligent vehicles.

INDEX TERMS Intelligent vehicle, emergency obstacle avoidance, safety distance model, trajectory planning, model predictive control.

I. INTRODUCTION

Among the three elements of human-vehicle-road traffic, humans are the most uncontrollable [1]. According to the U.S. National Highway Traffic Safety Administration, more than 88% of traffic accidents are caused by misjudgments or slow responses of drivers [2]. An emergency obstacle avoidance system that can reduce accidents caused by human factors and improve driving safety is one of the key technologies of intelligent vehicles that has attracted extensive attention [3], [4], [5]. An emergency obstacle avoidance system can process and analyze obstacle information, vehicle speed, the surrounding environment and other information. According to the obstacle avoidance strategy, the best obstacle avoidance method is reasonably selected and the corresponding action is completed by controlling the vehicle. Emergency obstacle avoidance mainly includes longitudinal braking obstacle avoidance and lateral steering obstacle avoidance.

Braking obstacle avoidance research mainly includes braking safety distance models and obstacle avoidance control strategies. The accuracy of the obstacle avoidance strategy is determined by whether the safety distance model is reasonable, and the effectiveness of obstacle avoidance strategy is determined by the accuracy of obstacle avoidance control. References [6] and [7] designed an emergency braking algorithm that took ramps into account to improve the performance of emergency obstacle avoidance systems

The associate editor coordinating the review of this manuscript and approving it for publication was Jie Gao.

on sloping roads. References [8], [9], and [10] proposed a braking obstacle avoidance strategy based on the collision safety time that improved the accuracy of obstacle avoidance. References [11] and [12] designed an emergency braking algorithm considering road adhesion coefficient that improved the adaptability of an emergency obstacle avoidance system on different roads. The above research was mainly focused on braking obstacle avoidance. When the speed is high or the road adhesion coefficient is low, the braking distance will be greatly increased. In these conditions, steering obstacle avoidance is a better choice.

Steering obstacle avoidance research mainly includes path planning and path tracking. Due to the nonlinearity of a vehicle, it is necessary to consider the stability of the vehicle in the course of lane changes [13], [14], [15]. References [16], [17], and [18] designed obstacle avoidance trajectory planning with the motion constraints of a vehicle to achieve reasonable lane change obstacle avoidance. References [19] and [20] designed an algorithm for path-tracking control based on the safety distance model to achieve the requirements of stable collision avoidance. References [21], [22], and [23] designed a corresponding controller for real-time steering obstacle avoidance and verified the effectiveness of the algorithm through experiments. The above research was mainly focused on steering obstacle avoidance.

Some scholars studied the coordinated steering and braking control of intelligent vehicles in emergency obstacles. Reference [24] considered the factors of obstacle vehicles to determine the priorities of steering and braking. When steering was the priority, the intervention of traffic elements in the side lane was considered, and then the best reasonable collision avoidance mode was selected. Reference [25] used an estimation of the road adhesion coefficient to calculate the safety warning distance of braking and steering for decision-making. Reference [26] considered the relative speed and relative acceleration combined with the road adhesion coefficient to determine the steering or braking collision avoidance. The above research was mainly focused on obstacle avoidance decision-making, and it ignored the handling stability and ride comfort in obstacle avoidance control.

In summary, this paper proposes a coordinated steering and braking control obstacle avoidance strategy, considering the handling stability and ride comfort, that can select the best obstacle avoidance mode according to the driving environment of a vehicle.

II. INTELLIGENT VEHICLE DYNAMICS MODEL

A. THREE DRGRFF OF FREEDOM (3-DOF) VEHICLE MODEL

The vehicle is actually a complex nonlinear system. The forces coupled with each other are complex in the driving process. In order to make the study of the vehicle dynamics simple, the following assumptions are made:

(1) Assuming that the vehicle runs on a flat road surface, and ignoring the vertical motion of the vehicle.
(2) Assuming that the tire is always in the sideslip range during driving, and ignoring the coupling of tire force.
(3) Assuming that the vehicle and the suspension are rigid bodies, and ignoring the effect of the suspension.
(4) Assuming that the vehicle only rolls during driving without sliding.
(5) Lateral and longitudinal aerodynamics are not considered.

A 3-DOF vehicle dynamics model with longitudinal, lateral and yaw motions is established as shown in Fig.1.

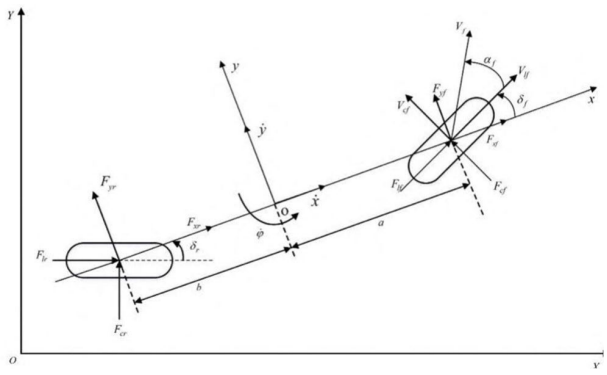

FIGURE 1. Vehicle 3-DOF model.

The dynamic equations of the vehicle can be derived as

$$\begin{cases} m\ddot{x} = m\dot{y}\dot{\varphi} + 2\left[C_{lf} + C_{cf}\left(\delta_f - \dfrac{\dot{y}+a\dot{\varphi}}{\dot{x}}\right)\delta_f + C_{lr}s_r\right] \\ m\ddot{y} = -m\dot{x}\dot{\varphi} + 2\left[C_{cf}\left(\delta_f - \dfrac{\dot{y}+a\dot{\varphi}}{\dot{x}}\right) + C_{cr}\dfrac{b\dot{\varphi}-\dot{y}}{\dot{x}}\right] \\ I\ddot{\varphi} = 2\left[aC_{cf}\left(\delta_f - \dfrac{\dot{y}+a\dot{\varphi}}{\dot{x}}\right) - bC_{cr}\dfrac{b\dot{\varphi}-\dot{y}}{\dot{x}}\right] \\ \dot{X} = \dot{x}\cos\varphi - \dot{y}\sin\varphi \\ \dot{Y} = \dot{x}\sin\varphi + \dot{y}\cos\varphi \end{cases} \tag{1}$$

where m is the total vehicle mass, $\dot{x}$ and $\ddot{x}$ are the longitudinal velocity and longitudinal acceleration, $\dot{y}$ and $\ddot{y}$ are the lateral velocity and lateral acceleration, I is the vehicle moment of inertia about the z-axis, φ and $\dot{\varphi}$ are the yaw angle and yaw rate respectively, a and b are the distance from the vehicle center of mass to the front and rear axle of the vehicle, C_l is the longitudinal stiffness of the tire; C_c is the lateral stiffness of the tire, δ_f is the front wheel steering angle.

B. LONGITUDINAL CONTROL VEHICLE MODEL

When the vehicle is at a constant speed, the equation of motion is:

$$F_t = F_w + F_f + F_i + F_j \tag{2}$$

where F_t is the driving force, F_w is the air resistance, F_f is the rolling resistance, F_i is the climbing resistance, and F_j is the acceleration resistance.

When the vehicle is in an accelerated state, the driving force is:

$$F_t = ma - \sum F\,(v) \tag{3}$$

where $\sum F(v)$ is the sum of resistance in driving. To facilitate the calculation, just considering rolling resistance and air resistance, that is:

$$\sum F(v) = F_w + F_f = \frac{1}{2}C_D A_a \rho v^2 + mgf \tag{4}$$

where C_D is the air resistance coefficient, A_a is the windward area, ρ is the air density and f is the rolling resistance coefficient.

The relationship between the driving force and the motor torque is:

$$F_t = \frac{T_{motor}}{r} i_0 \eta_t \tag{5}$$

where T_{motor} is the driving torque of the motor, r is the rolling radius of the wheel, i_0 is the transmission ratio of the main reducer, η_t is the mechanical efficiency of the transmission system.

Combining equation (3) to (5), the driving torque of the motor can be obtained:

$$T_{motor} = \frac{r\left(ma + \frac{1}{2}C_D A_a \rho v^2 + mgf\right)}{i_0 \eta_t} \tag{6}$$

When the vehicle is braking, the desired braking force can be obtained:

$$F_d = -ma_{des} - \frac{1}{2}C_D A_a \rho v^2 - mgf \tag{7}$$

where a_{des} is the desired acceleration.

If the desired braking force is within the maximum braking force allowed on the ground, there is a linear relationship between the braking force and the pressure in the braking pipeline. The desired brake pipeline pressure can be described as follows:

$$P_{des} = \frac{-ma_{des} - \frac{1}{2}C_D A_a \rho v^2 - mgf}{k} \tag{8}$$

where k is the linear coefficient between braking force and braking pipeline, and P_{des} is the desired pressure of braking pipeline.

When the driving force of the vehicle is zero, only air resistance and friction resistance in the longitudinal direction, the maximum acceleration is called the maximum sliding deceleration. The maximum sliding deceleration can be described as:

$$a_s = \frac{F_w + F_i}{m} = \frac{C_D A_a \rho v^2 + 2mgf}{2m} \tag{9}$$

To avoid frequent switching of driving mode and braking mode, a threshold on both sides of the maximum sliding acceleration Δa is set. According to experience, generally $\Delta a = 0.1$ m/s^2. The driving and braking switching strategy of the vehicle is established as shown in Fig 2.

The driving and braking switching strategy of vehicle is designed as follows:

(1) When the desired acceleration is less than $a_s - \Delta a$, the vehicle performs a braking mode and decelerates;

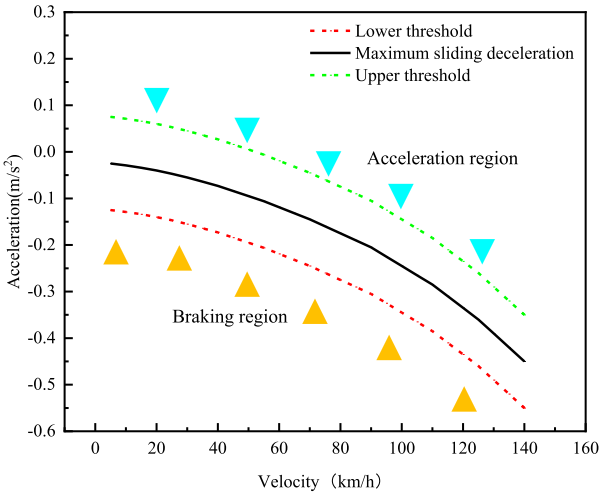

FIGURE 2. Driving and braking switching strategy of vehicle.

(2) When the desired acceleration is greater than $a_s + \Delta a$, the vehicle performs a driving mode and accelerates;

(3) When the desired acceleration is at $[a_s - \Delta a, a_s + \Delta a]$, the state of the vehicle remains unchanged.

III. DESIGN OF INTELLIGENT VEHICLE EMERGENCY OBSTACLE AVOIDANCE SYSTEM

A. DESIGN OF EMERGENCY OBSTACLE AVOIDANCE SYSTEM

The emergency obstacle avoidance system includes environment perception module, planning and decision module and execution control module. The emergency obstacle avoidance system designed in this paper is shown in Figure 3.

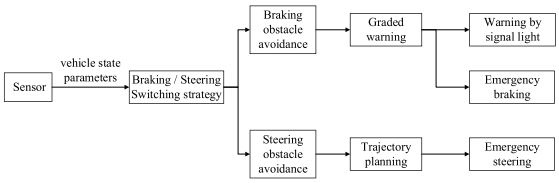

FIGURE 3. Emergency obstacle avoidance system.

The obstacle avoidance strategy designed in this paper is shown in Figure 4.

When the intelligent vehicle detects an obstacle vehicle ahead, the minimum safety distance required for braking obstacle avoidance and steering obstacle avoidance is calculated. When the real-time vehicle distance d_r between the host vehicle and the obstacle vehicle is greater than the maximum value of the steering safety distance d_s and the braking safety distance d_b, that is, when $d_r > \max\{d_b, d_s\}$, braking or steering can be achieved for obstacle avoidance and safe driving. Considering the convenience of driving operation, the braking obstacle avoidance is selected; When the real-time vehicle distance is greater than the steering safety distance and less than the braking safety distance, that is, when

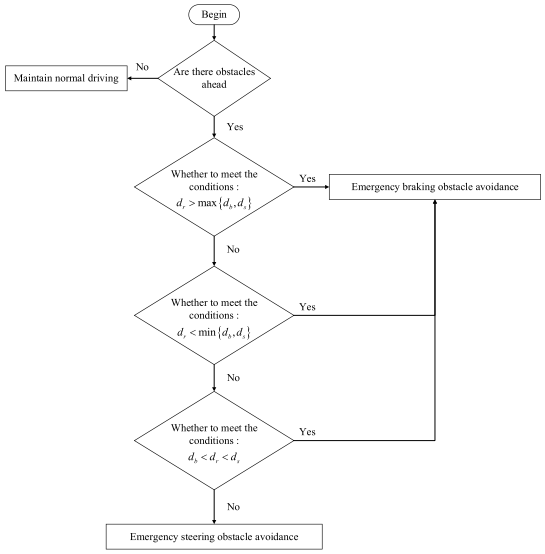

FIGURE 4. Obstacle avoidance strategy.

$d_b < d_r < d_s$, the braking obstacle avoidance cannot meet the obstacle avoidance requirements, and steering obstacle avoidance is selected; When $d_r < \{d_b, d_s\}$, braking and steering cannot achieve obstacle avoidance, and braking is selected to minimize collisions and reduce casualties and property losses.

B. EMERGENCY BRAKING OBSTACLE AVOIDANCE

In the process of braking obstacle avoidance, the change curve of braking acceleration with time is shown in Figure 5.

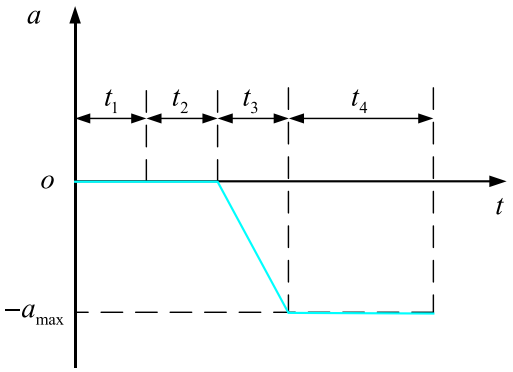

FIGURE 5. Relationship between braking acceleration and time.

t_1-Driver's reaction time;t_2- Brake coordination time;
t_3- Brake force increase time; t_4-Continuous braking time;
a_{max}- Maximum braking acceleration
The braking distance S_1 in t_1 and t_2 is:

$$S_1 = v_1(t_1 + t_2) \tag{10}$$

The braking distance S_2 in t_3 is:

$$S_2 = v_1 t_3 - \frac{1}{6} a_{max} t_3^2 \tag{11}$$

The braking distance S_3 in t_4 is:

$$S_3 = \frac{v_1^2}{2a_{max}} - \frac{v_1 t_3}{2} + \frac{1}{8} a_{max} t_3^2 \tag{12}$$

The total braking distance during the braking process is:

$$S = v_1(t_1 + t_2 + \frac{t_3}{2}) + \frac{v_1^2}{2a_{max}} - \frac{1}{24} a_{max} t_3^2 \tag{13}$$

The relationship between the road adhesion coefficient and the maximum acceleration is:

$$a_{max} = \mu_{max} g \tag{14}$$

where μ_{max} is the maximum adhesion coefficient of the current road.

In general, the value of t_1 is 1 seconds, the values of t_2 and t_3 are determined by the performance of the braking system, the value of t_2 is 0.2 seconds, the value of t_3 is about 0.04 seconds [27], so the last term in formula (13) can be ignored.

When the obstacle vehicle is stationary or driving at a constant speed, which is far greater than the speed of the host vehicle, that is, when $v_2 \gg v_1$, the two vehicles will not collide; When the speed of the obstacle vehicle is less than the speed of the host vehicle, that is, when $v_2 < v_1$, the two vehicles may collide, and the distance between the two vehicles becomes smaller with the passage of time. The host vehicle must brake until the two vehicles are at a same speed with a certain safe distance. The distance traveled by the vehicle is:

$$d_1 = v_1(t_1 + t_2 + \frac{t_3}{2}) + \frac{v_1^2 - v_2^2}{2a_{max}} \tag{15}$$

$$d_2 = v_2(t_1 + t_2 + t_3 + \frac{v_1 - a_{max} t_3 - v_2}{a_{max}}) \tag{16}$$

where d_1 is the distance traveled by the host vehicle, d_2 is the distance traveled by the obstacle vehicle. The safety warning distance d_b between the two vehicles can be obtained:

$$\begin{aligned} d_b &= d_1 - d_2 + d_0 \\ &= (v_1 - v_2)(t_1 + t_2) - \frac{v_1 t_3}{2} + \frac{v_1^2 - 2v_1 v_2}{2a_{max}} + d_0 \end{aligned} \tag{17}$$

where d_0 is the minimum safe distance between the two vehicles after the host vehicle decelerates, generally its value is 2-5 m, and 3 m is selected in this paper.

The difference between the safety warning distance and the distance traveled in the driver's reaction time is the critical braking distance d_{bl}, that is:

$$d_{bl} = (v_1 - v_2) t_2 - \frac{v_1 t_3}{2} + \frac{v_1^2 - 2v_1 v_2}{2a_{max}} + d_0 \tag{18}$$

When the obstacle vehicle brakes, the host vehicle must also brake to ensure a certain safety distance between the two vehicles. Assuming that the host vehicle brakes at the maximum braking acceleration until the two vehicles are at

the same speed v, the safety warning distance between the two vehicles is described as:

$$d_b = d_1 - d_2 + d_0 = v_1\left(t_1 + t_2 + \frac{t_3}{2}\right) + \frac{a_2 v_1^2 + a_1 v_2^2 - (a_1 + a_2)\, v^2}{2a_1 a_2} + d_0 \tag{19}$$

The critical braking distance is derived as:

$$d_{bl} = v_1\left(t_2 + \frac{t_3}{2}\right) + \frac{a_2 v_1^2 + a_1 v_2^2 - (a_1 + a_2)\, v^2}{2a_1 a_2} + d_0 \tag{20}$$

The environmental perception module of the obstacle avoidance system monitors the relative distance d_r between the vehicles in real-time, and the decision control module compares d_r, d_b and d_{bl} to establish a graded warning. When $d_r > d_b$, there is no collision risk, the system does not carry out an early warning, and the warning level is Level 0. When $d_{bl} < d_r < d_b$, the warning level is Level 1, and the system uses the signal light, voice broadcast or another method to remind the driver to take action. When $d_r < d_{bl}$, the warning level is Level 2, and the system performs emergency braking to avoid obstacles.

C. EMERGENCY STEERING OBSTACLE AVOIDANCE

1) EMERGENCY STEERING SAFETY DISTANCE MODEL

When the vehicle performs emergency steering to avoid obstacles, the lane-changing time is short and the longitudinal speed of the vehicle is fast in most cases. It can be considered that the longitudinal speed of the vehicle is constant in the lane changing process and the initial lateral velocity is zero with an acceleration a_y.

When the obstacle vehicle is stationary or driving at a constant speed that is less than the host vehicle's speed, that is, when $v_2 < v_1$, a collision may occur. With the passage of time, the distance between the two vehicles becomes smaller and it is necessary to steer to avoid obstacles. The minimum longitudinal safety distance is described as:

$$d_s = v_1 t_c - v_2 t_c + d_0 \tag{21}$$

When the obstacle vehicle decelerates at the maximum deceleration, the minimum longitudinal safety distance is described as:

$$d_s = v_1 t_c - \left(v_2 t_c - \frac{1}{2} a_2 t_c^2\right) + d_0 \tag{22}$$

2) EMERGENCY STEERING TRAJECTORY PLANNING

There are many kinds of trajectory planning methods suitable for different scenes and conditions. The commonly used trajectory planning methods include B-spline curve trajectory planning [28], the artificial potential field method [29], an A * algorithm [30], and a rapidly-exploring random tree algorithm [31], [32]. The vehicle lane changing trajectory fitted with the fifth-degree polynomial has the advantage of the continuous and smooth curvature of each point. Therefore, in this research the fifth-degree polynomial is selected to plan the lane-changing trajectory.

The general form of the fifth-degree polynomial with the longitudinal displacement of the lane change as the independent variable and the lateral displacement of the lane change as the dependent variable is:

$$y(x) = a_0 + a_1 x + a_2 x^2 + a_3 x^3 + a_4 x^4 + a_5 x^5 \tag{23}$$

The lateral velocity and acceleration at the beginning and end of lane change are zero, so the function boundary condition is:

$$y(0) = 0, \dot{y}(0) = \dot{y}(x_e) = 0, \ddot{y}(0) = \ddot{y}(x_e) = 0 \tag{24}$$

The fifth-degree polynomial is derived as:

$$y(x) = y_e\left[10\left(\frac{x}{x_e}\right)^3 - 15\left(\frac{x}{x_e}\right)^4 + 6\left(\frac{x}{x_e}\right)^5\right] \tag{25}$$

where x_e is the longitudinal displacement required to complete lane change collision avoidance, y_e is the lateral displacement required to complete the lane change collision avoidance.

Assuming that the longitudinal speed of the vehicle v_x is constant in the lane changing process, and x_e is obtained as:

$$x_e = v_x t_e \tag{26}$$

where t_e is the time required to complete the lane change.

The lane-changing collision avoidance model with time as a variable can be obtained:

$$y(t) = y_e\left[10\left(\frac{t}{t_e}\right)^3 - 15\left(\frac{t}{t_e}\right)^4 + 6\left(\frac{t}{t_e}\right)^5\right] \tag{27}$$

The lane-changing obstacle avoidance trajectory is shown in figure 6.

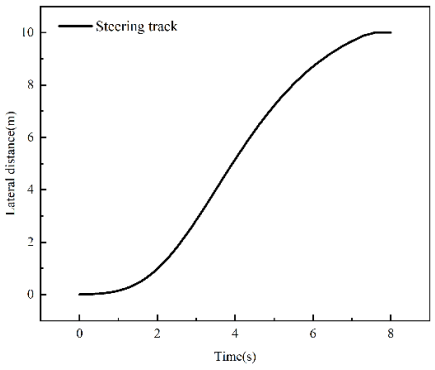

FIGURE 6. Lane-changing obstacle avoidance trajectory.

3) EMERGENCY STEERING CONSTRAINTS

a: LATERAL ACCELERATION CONSTRAINT

The lateral acceleration of the vehicle a_y in the lane changing process can be obtained by taking two derivatives of equation (27):

$$a_y(t) = y(t) = \frac{60 y_e}{t_e}\left(t_e^2 t - 3t_e t^2 + 2t^3\right) \tag{28}$$

It can be found from equation (28) that lateral acceleration is related to the lane-changing time and the lateral distance. The greater the lateral acceleration, the shorter the time required to complete obstacle avoidance. However, an excessive lateral acceleration will cause discomfort to the driver and affect the stability of the vehicle.

The lateral acceleration is a cubic polynomial with respect to the lane change time, and there is an extreme value in $(0,\ t_e)$. The first derivative of lateral acceleration is:

$$a_y(t) = \frac{60y_e}{t_e^5}\left(t_e^2 - 6t_e t + 6t^2\right) \tag{29}$$

The maximum lateral acceleration can be obtained:

$$a_{y\max} = \frac{10\sqrt{3}\,y_e}{3t_e^2} \tag{30}$$

The lateral acceleration is also constrained by the road adhesion. The maximum lateral acceleration should not exceed the road adhesion coefficient when the vehicle is steering, that is, the maximum lateral acceleration should satisfy $a_{y\max} < \mu g$. When the lateral acceleration is high in the limit lane change condition, there is:

$$a_{y\max} \ll 0.67\mu g \tag{31}$$

When the lateral acceleration is too large, it is easy to cause vehicle instability and rollover. When the lateral acceleration is too small, a larger longitudinal safety distance is required, that is contrary to the purpose of obstacle avoidance. The lateral acceleration is generally not more than 0.35 g. The steering obstacle avoidance studied in this paper is a relatively emergency condition, considering the ride comfort, the limited acceleration is not more than 0.30 g. In order to ensure that the lateral acceleration is always within the allowable range in the lane changing process, there is:

$$t_e \geq t_{a_{y\max}} = \sqrt{\frac{10\sqrt{3}\,y_e}{3a_{y\max}}} \tag{32}$$

b: SECURITY CONSTRAINTS

The steering obstacle avoidance trajectory is shown in Figure 7.

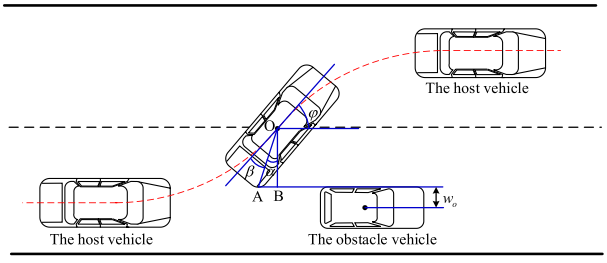

FIGURE 7. Schematic diagram of safe lane changing and collision avoidance.

Where, O is the center of mass of the vehicle, A is the right rear point of the vehicle, w_o is half the width of the obstacle vehicle, φ is the yaw angle, and L_{OA} is the distance from the vehicle center of mass to the right rear point.

In the lane changing process, the easiest point to collide with the obstacle vehicle is the right front and rear points of the host vehicle, and the right rear point is the last collision point. Therefore, it is only necessary to ensure that the right rear point of the host vehicle crosses the obstacle vehicle within the limited longitudinal distance [33]. According to reference [33], the critical collision time t_c of the vehicle can be obtained:

$$w_o = y_e\left[10\left(\frac{t_c}{t_e}\right)^3 - 15\left(\frac{t_c}{t_e}\right)^4 + 6\left(\frac{t_c}{t_e}\right)^5\right] - L_{OA}\cos\left(90 - \varphi_{\max} - \beta\right) \tag{33}$$

In order to ensure safety in the lane changing process, the time t_e to complete lane changing must be greater than the time t_c of critical collision.

c: ROAD BOUNDARY CONSTRAINTS

In the process of steering obstacle avoidance, the vehicle needs to abide by the traffic law, and it must be ensured that the vehicle is always within the road boundary and cannot exceed the road solid line or the road boundary, that is:

$$y_e + w_o < \{y_s, y_b\} \tag{34}$$

where y_s is the lateral distance from the center line of the vehicle to the solid line of the road, y_b is the lateral distance from the center line of the vehicle to the road boundary.

D. TRAJECTORY TRACKING

To verify the effectiveness of the steering obstacle avoidance trajectory planning method, it is necessary to consider that the vehicle can accurately track the obstacle avoidance path, and the driving safety and ride comfort can be satisfied. Therefore, the maximum lateral acceleration, the roll angle and the yaw angle of the vehicle in the steering process should be within the allowable range. The model predictive control (MPC) algorithm can constraint the vehicle intermediate state, and determine the importance of parameters in the tracking control process with different weight coefficients, which is suitable for solving multi-constrained problems [34], [35]. The principle of model predictive control is shown in Figure 8.

1) LINEAR PREDICTION MODEL

The state quantity of vehicle is described as $\xi = [X, Y, \dot{x}, \dot{y}, \varphi, \dot{\varphi}]$, and the control quantity is $u = \delta_f$, where X and Y are the coordinate value of longitudinal and lateral displacement in the geodetic coordinate system, $\dot{x}$ is the longitudinal velocity of the vehicle center of mass, $\dot{y}$ is the lateral velocity of the vehicle center of mass, φ is the yaw angle, $\dot{\varphi}$ is the yaw rate, δ_f is the front wheel steering angle.

The equation of the state and control quantities at each moment on the trajectory is:

$$\dot{\xi}_r = f(\xi_r, u_r) \tag{35}$$

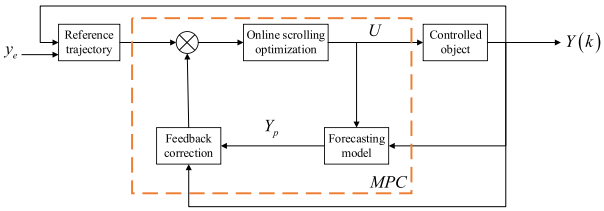

FIGURE 8. Principle of Model Predictive Control.

By Taylor expansion, it can be obtained:

$$\Delta\dot{\xi} = A(t) \cdot \Delta\xi + B(t) \cdot \Delta u \tag{36}$$

where equations $A(t)$, $B(t)$, as shown at the bottom of the page.

By discretizing the continuous form state equation through the first-order difference quotient, it can be obtained:

$$\xi(k+1) = A(k)\,\xi(k) + B(k)\,u(k) \tag{37}$$

To realize the prediction function, there is:

$$p(k|t) = \begin{bmatrix} \xi(k|t) \\ u(k-1|t) \end{bmatrix} \tag{38}$$

$$p(k+1|t) = \tilde{A}(k)\,p(k) + \tilde{B}(k)\,\Delta u(k) \tag{39}$$

where $\tilde{A}(k) = \begin{bmatrix} A(k) & B(k) \\ O_{m\times n} & I_m \end{bmatrix}$, $\tilde{B}(k) = \begin{bmatrix} B(k) \\ I_m \end{bmatrix}$, m is the number of control variables, n is the number of state variables.

2) OBJECTIVE FUNCTION DESIGN

In order to prevent sudden changes in the front wheel angle during trajectory tracking, the increment of the control variable can be controlled to ensure that the front wheel angle is always within the allowable variation range in each cycle. The control objective function is:

$$\begin{aligned} J(k) = &\sum_{i=1}^{N_p} \left[\eta(k+i) - \eta_{ref}(k+i)\right]^T \\ &Q\left[\eta(k+i) - \eta_{ref}(k+i)\right] \\ &+ \sum_{i=1}^{N_c-1} \Delta u(k+i)\,R\Delta u(k+i) + \rho\varepsilon^2 \end{aligned} \tag{40}$$

where η_{ref} is the expected output of the planned trajectory, Δu is the front wheel angle increment, Q and R are the weight matrices, ρ is a weight coefficient, ε is a relaxation factor to avoid the situation that there is no solution due to too tight constraint.

The following constraints are established during control.

a: SIDESLIP ANGLE CONSTRAINT

The sideslip angle is one of the important indexes that affect the stability performance of the vehicle. When the vehicle is on the road with a high adhesion coefficient, the sideslip angle limit can reach ± 12°. When the vehicle is on the road with a low adhesion coefficient, the sideslip angle limit is ± 2°. Therefore, the range of the sideslip angle is described as:

$$-12^\circ < \beta < 12^\circ \tag{41}$$

$$-2^\circ < \beta < 2^\circ \tag{42}$$

b: TIRE SLIP ANGLE CONSTRAINT

There is a linear relationship between the slip angle and the lateral force when the tire slip angle is within 5°. Under the assumption of a small angle, the range of the tire lateral force is described as:

$$-2.5^\circ < \alpha < 2.5^\circ \tag{43}$$

c: MAXIMUM LATERAL ACCELERATION CONSTRAINT

In order to ensure the stability of the vehicle in the lane changing process, the range of the lateral acceleration is described as:

$$|a_y| \le 0.3\,g \tag{44}$$

In order to ensure there is an optimal solution, the range of lateral acceleration is described as:

$$a_{y,\min} - \varepsilon \le a_y \le a_{y,\max} + \varepsilon \tag{45}$$

d: FRONT WHEEL STEERING ANGLE AND ITS INCREMENTAL CONSTRAINT

When the input of the front wheel steering angle is too large, it will make the vehicle run-out, and even rollover. According to experience, the range of the front wheel steering angle and its increment constraint are described as:

$$-25^\circ < \delta < 25^\circ \tag{46}$$

$$-0.47^\circ < \Delta\delta < 0.47^\circ \tag{47}$$

$$A(t) = \frac{\delta f}{\delta \xi} = \begin{bmatrix} \frac{-2(C_{cf}+C_{cr})}{m\dot{x}} & \frac{\delta f\dot{y}}{\delta\dot{x}} & 0 & -\dot{x} + \frac{2(bC_{cr}-aC_{cf})}{m\dot{x}} & 0 & 0 \\ \dot{\phi} - \frac{2c_{cf}\delta_f}{m\dot{x}} & \frac{\delta f\dot{x}}{\delta\dot{x}} & 0 & \dot{y} - \frac{2aC_{cf}\delta_f}{m\dot{x}} & 0 & 0 \\ 0 & 0 & 0 & 1 & 0 & 0 \\ \frac{2(bC_{cr}-aC_{cf})}{I_s\dot{x}} & \frac{\delta f\dot{\phi}}{\delta\dot{x}} & 0 & \frac{2(a^2C_{cf}-b^2C_{cr})}{I_s\dot{x}} & 0 & 0 \\ \cos\phi & \sin\phi & \dot{x}\cos\phi - \dot{y}\sin\phi & 0 & 0 & 0 \\ -\sin\phi & \cos\phi & -\dot{y}\cos\phi - \dot{x}\sin\phi & 0 & 0 & 0 \end{bmatrix}$$

$$B(t) = \frac{\partial f}{\partial u} = \begin{bmatrix} \frac{2C_{cf}}{m} & \frac{2C_{cf}\left(2\delta_f - \frac{\dot{y}-b\dot{\varphi}}{\dot{x}}\right)}{m} & 0 & \frac{2aC_{cf}}{I_s} & 0 & 0 \end{bmatrix}$$

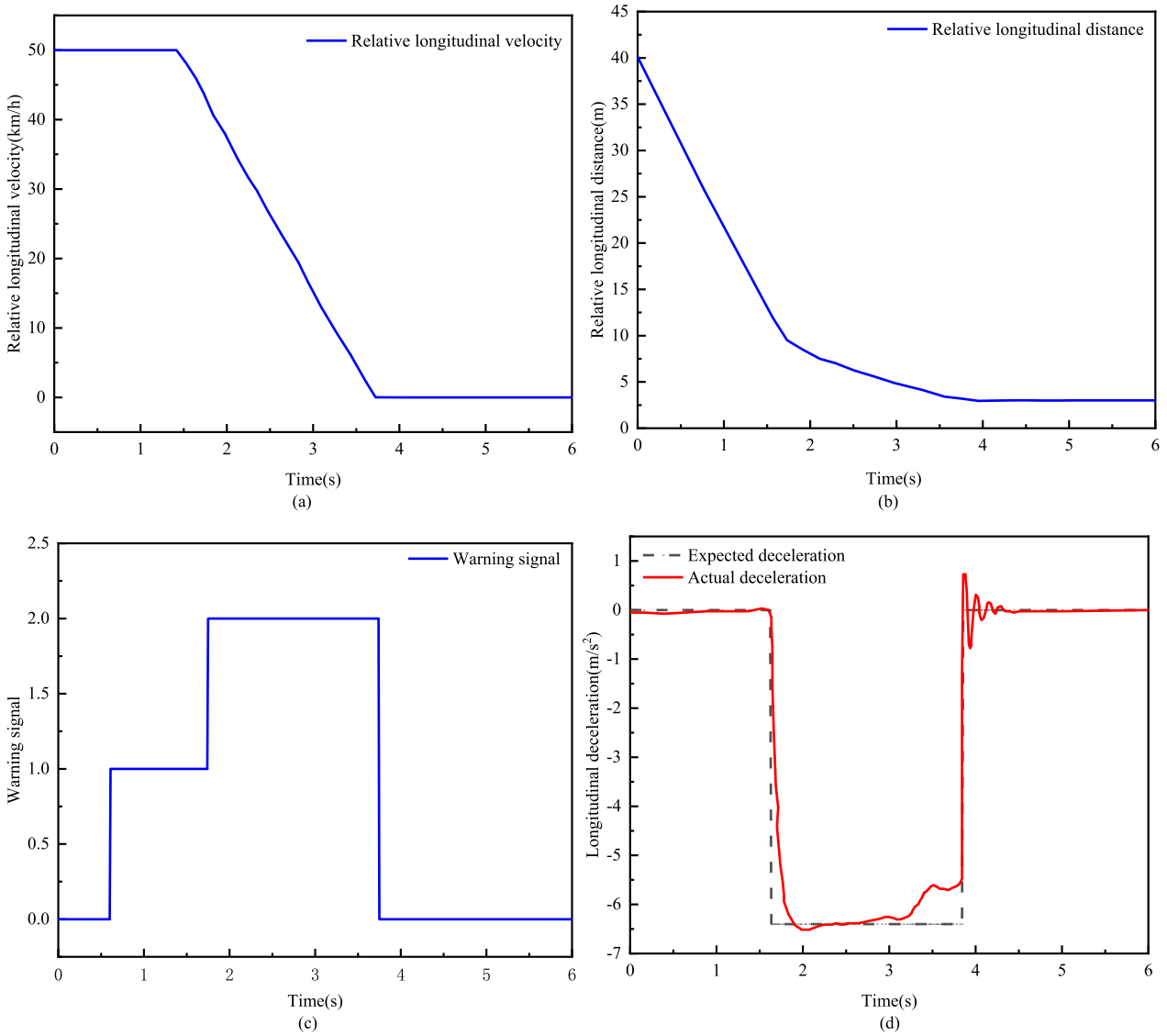

FIGURE 9. Simulation results of emergency braking: (a) Relative velocity; (b) Relative distance; (c) Braking deceleration; (d) Warning signals.

In order to reduce the computation time, the solution of model predictive control is transformed into a standard quadratic programming problem. The general format of quadratic programming with inequality and upper and lower bound constraints is:

$$\min \frac{1}{2} x^T H x + f^T x \tag{48}$$

$$s.t. \quad Fx \le b$$

$$lb \le x \le ub \tag{49}$$

where H is a positive definite Hessian matrix, lb and ub are the lower and upper bounds of x respectively.

Combining objective functions and constraints, the MPC-based mathematical optimization problem is described as:

$$\min \left[sc, \min \Delta U^T, \varepsilon \right]^T H \left[\Delta U, \varepsilon \right] + G \left[\Delta U^T, \varepsilon \right]$$

$$\begin{aligned} &\Delta U_{\min} \le \Delta U_k \le \Delta U_{\max} \\ &\Delta U_{\min} - U_k \le M \Delta U_{k+1} \le \Delta U_{\max} - U_k \\ &y_{hc,\min} \le y_{hc} \le y_{hc,\max} \\ &y_{hc,\min} - \varepsilon \le y_{hc} \le y_{hc,\max} - \varepsilon \\ &\varepsilon > 0 \end{aligned} \tag{50}$$

The control increment sequence in the control time domain can be obtained:

$$\Delta U = \left[\Delta u \left(k \mid t \right), \Delta u \left(k+1 \mid t \right), \cdots, \Delta u \left(k+N_c-1 \mid t \right) \right]^T \tag{51}$$

Add the first value of the increment sequence to the control at the previous time, it can be obtained:

$$u \left(k \mid t \right) = u \left(k-1 \mid t \right) + \Delta u \left(k \mid t \right) \tag{52}$$

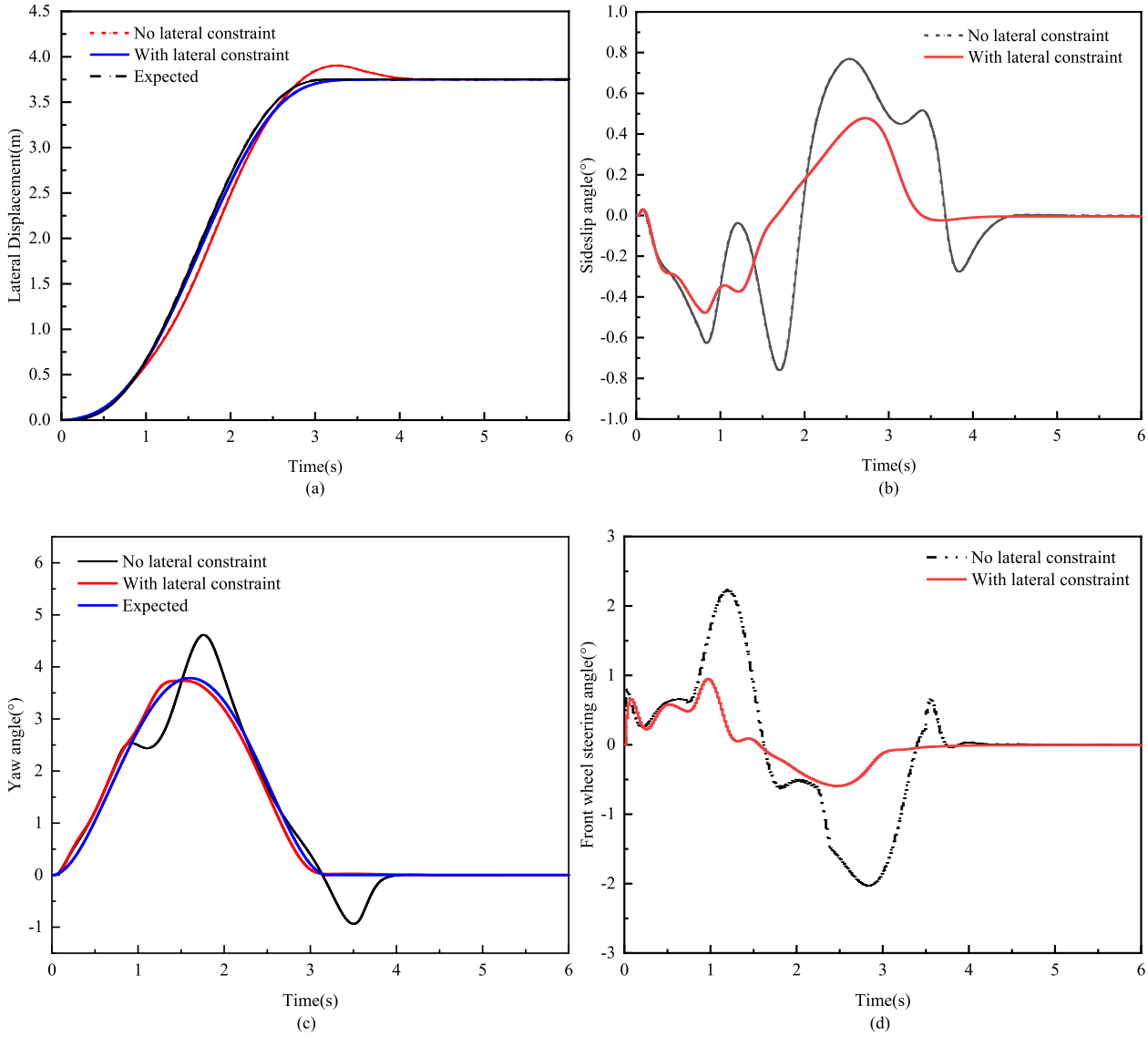

FIGURE 10. Simulation results of emergency steering: (a) Path tracking; (b) Sideslip angle; (c)Yaw angle; (d) Front wheel steering angle.

Equation (51) is the updated control, and at the next time equation (50) is resolved to obtain a new control increment sequence, that is circulated until the trajectory tracking is completed.

IV. CO-SIMULATION RESULTS

To verify the effectiveness of the proposed emergency obstacle avoidance control strategy, MATLAB / CARSIM are used to establish a co-simulation test. The specific basic parameters of the vehicle are shown in Table 1.

A. EMERGENC BRAKING OBSTACLE AVOIDANCE VERIFICATION

The vehicle is set at a speed of 50 km/h on the road with the adhesion coefficient of 0.8, and there is a stationary obstacle 50 m ahead. According to the calculation of the emergency obstacle avoidance system, the minimum longitudinal distance required for braking obstacle avoidance is 18.12 m, and the longitudinal distance required for steering obstacle avoidance is 29.17 m. At this time, both methods can be selected to achieve obstacle avoidance, but the longitudinal distance required for braking obstacle avoidance is smaller, so the braking obstacle avoidance is selected under the condition. The simulation results are shown in Figure 9.

It can be found from Fig. 9(a)(b)(c) that the vehicle receives a level-1 warning signal at 0.61 seconds to remind the driver to pay attention to the obstacles ahead. However, due to the driver's failure or incorrect operation, the vehicle speed does not change. The system sends a level-2 warning signal at 1.75 seconds. At this time, the obstacle avoidance system intervenes to start emergency braking, the vehicle stops at about 3.74 seconds and maintains a safe reserved distance

TABLE 1. Basic parameters of the vehicle.

Variables	Unit	Value
Total mass	kg	1350
Distance from center of mass to front axle	m	1.056
Distance from center of mass to rear axle	m	1.555
Center of mass moment of inertia	$Kg \cdot m^2$	2523
Front axle side deflection stiffness	$N \cdot rad^{-1}$	-96196
Rear axle side deflection stiffness	$N \cdot rad^{-1}$	-99078
Centroid height	m	0.540
Tire radius	m	0.316
Distance between front wheels	m	1.540
Distance between rear wheels	m	1.540

of 3 m from the obstacle vehicle in front. It can be found from Fig. 9(d) that the braking deceleration fluctuates when the vehicle starts braking, but the difference from the expected acceleration is not large, which can meet the demand.

B. EMERGENCY STEERING OBSTACLE AVOIDANCE VERIFICATION

The host vehicle is set at a speed of 120 km/h on the road with the adhesion coefficient of 0.40, and there is an obstacle vehicle 85 m ahead, which is braking at the initial speed of 30 km/h with the maximum deceleration. According to the calculation of the emergency obstacle avoidance system, the minimum longitudinal distance required for braking obstacle avoidance is 172.24 m, and the minimum longitudinal distance required for steering obstacle avoidance is 79.65 m. At this time, only steering obstacle avoidance can achieve safe driving, so the emergency steering obstacle avoidance is selected. The simulation results are shown in Fig. 10.

It can be found from Fig. 10(a) that, both the controller with and without lateral constraint can track the designed path well in the initial stage of tracking, but the controller without lateral constraint has a large tracking error in the middle and end stages of lane changing, and the maximum error is 0.25 m. Compared with the controller without lateral constraint, the controller with lateral constraint can track the designed path better, the maximum error is 0.09 m.

It can be found from Fig. 10(b) that, both side-slip angles of the center of mass are in the constraint range of $-2°$ to $2°$ on the road with the low adhesion coefficient. Compared with the controller without lateral constraint, the controller with lateral constraint has smaller fluctuation, which shows that the controller with lateral constraint can achieve stability faster.

It can be found from Fig.10(c) that, compared with the controller with lateral constraint, the controller without lateral constraint has a great fluctuation at the middle and the end of lane changing in the yaw angle. The controller with lateral constraint is essentially matches the expected value in the yaw angle.

It can be found from Fig. 10 (d) that, both the front wheel steering angles are in the constraint range of $-25°$ to $25°$. Compared with the controller without lateral constraint, the controller with lateral constraint has a small fluctuation in the front wheel steering angle, which shows that the controller with lateral constraint has better handling stability.

V. CONCLUSION

(1) The longitudinal control model of the intelligent vehicle including driving system model, the braking system model and driving and braking switching strategy is established. The braking safety distance model based on the braking process and the steering safety distance model with multiple constraints are established. The Emergency obstacle avoidance decision is designed. By calculating and comparing the longitudinal distance required for steering obstacle avoidance and braking obstacle avoidance, the method with a smaller longitudinal distance is selected as the obstacle avoidance priority, so that the intelligent vehicle can select the appropriate obstacle avoidance method under different working conditions.

(2) The emergency braking obstacle avoidance scenario is set up for simulation. The results show that the intelligent vehicle can perform emergency obstacle avoidance according to the safe distance. During the test, as the longitudinal safety distance between the two vehicles gradually decreases, the vehicle starts to brake after receiving the secondary signal, and maintains a safe reserved distance of 3 m from the front obstacle vehicle.

(3) The emergency steering obstacle avoidance scenario is set up for simulation. The results show that the designed control strategy can select a reasonable obstacle avoidance method under the current working condition. Compared with the unconstrained controller, the trajectory tracking controller with constraints has a better tracking effect on the desired path, and the maximum error of lateral displacement can be reduced to 0.09 m, which improves the handling stability of the vehicle. The sideslip angle and the yaw rate are reduced, which can better control the change of the vehicle attitude and improve the ride comfort.

REFERENCES

[1] J. Wang, J. Wu, and Y. Li, "The driving safety field based on driver–vehicle–road interactions," *IEEE Trans. Intell. Transp. Syst.*, vol. 16, no. 4, pp. 2203–2214, Aug. 2015, doi: 10.1109/TITS.2015.2401837.

[2] H. Li, J. Li, Z. Su, X. Wang, and J. Luo, "Research on active obstacle avoidance control strategy for intelligent vehicle based on active safety collaborative control," *IEEE Access*, vol. 8, pp. 183736–183748, 2020, doi: 10.1109/ACCESS.2020.3029042.

[3] U. Rosolia, S. De Bruyne, and A. G. Alleyne, "Autonomous vehicle control: A nonconvex approach for obstacle avoidance," *IEEE Trans. Control Syst. Technol.*, vol. 25, no. 2, pp. 469–484, Mar. 2017, doi: 10.1109/TCST.2016.2569468.

[4] L. Li, Y. Lu, R. Wang, and J. Chen, "A three-dimensional dynamics control framework of vehicle lateral stability and rollover prevention via active braking with MPC," *IEEE Trans. Ind. Electron.*, vol. 64, no. 4, pp. 3389–3401, Apr. 2017, doi: 10.1109/TIE.2016.2583400.

[5] A. Eskandarian, C. Wu, and C. Sun, "Research advances and challenges of autonomous and connected ground vehicles," *IEEE Trans. Intell. Transp. Syst.*, vol. 22, no. 2, pp. 683–711, Feb. 2021, doi: 10.1109/TITS.2019.2958352.

[6] G. Kim, H. Mun, and B. Kim, "Performance of AEB system on a slope using an extended Kalman filter," *Int. J. Softw. Eng. Knowl. Eng.*, vol. 29, no. 7, pp. 955–969, Jul. 2019, doi: 0.1142/S0218194019400084.

[7] H. Kim, K. Shin, I. Chang, and K. Huh, "Autonomous emergency braking considering road slope and friction coefficient," *Int. J. Automot. Technol.*, vol. 19, no. 6, pp. 1013–1022, Dec. 2018, doi: 10.1007/s12239-018-0098-9.

[8] M. Fu, "Research on autonomous emergency braking control algorithms based on visual sensors," *J. Chongqing Univ. Technol.*, vol. 33, no. 12, pp. 55–60, Dec. 2019, doi: 10.3969/j.issn.1674-8425(z).2019.12.008.

[9] Y. Z. Hu, X. C. Yang, X. Liu, and L. Huang, "Hierarchic braking strategy for active collision avoidance and its verification based on drivers characteristics," *Automot. Eng.*, vol. 41, no. 3, pp. 298–306, Jun. 2019.

[10] F. C. Lan, M. Yu, S. C. Li, and J. Q. Chen, "Research on hierarchical control strategy for automatic emergency braking system with consideration of time-to-collision," *Automot. Eng.*, vol. 42, no. 2, pp. 206–214, Aug. 2020, doi: 10.19562/j.chinasae.qcgc.2020.02.010.

[11] B. Zhu, Q. Piao, J. Zhao, J. Wu, and W. W. Deng, "Vehicle longitudinal collision warning strategy based on road adhesive coefficient estimation," *Automot. Eng.*, vol. 38, no. 4, pp. 446–452, Jul. 2016, doi: 10.19562/j.chinasae.qcgc.2016.04.009.

[12] T. Chen, K. Liu, Z. Wang, G. Deng, and B. Chen, "Vehicle forward collision warning algorithm based on road friction," *Transp. Res. D, Transp. Environ.*, vol. 66, pp. 49–57, Jan. 2019, doi: 10.1016/j.trd.2018.04.017.

[13] F. Lai and X. Ye, "Research on feedforward and feedback tracking control for automatic emergency steering collision avoidance in vehicle high-speed driving," *Automot. Eng.*, vol. 42, no. 10, pp. 1401–1411, Mar. 2021.

[14] K. Lee and D. Kum, "Collision avoidance/mitigation system: Motion planning of autonomous vehicle via predictive occupancy map," *IEEE Access*, vol. 7, pp. 52846–52857, 2019, doi: 10.1109/ACCESS.2019.2912067.

[15] J. Tian, J. Ding, Y. Tai, and N. Chen, "Hierarchical control of nonlinear active four-wheel-steering vehicles," *Energies*, vol. 11, no. 11, p. 2930, Oct. 2018, doi: 10.3390/en11112930.

[16] J. Ji, A. Khajepour, W. W. Melek, and Y. Huang, "Path planning and tracking for vehicle collision avoidance based on model predictive control with multiconstraints," *IEEE Trans. Veh. Technol.*, vol. 66, no. 2, pp. 952–964, Apr. 2017, doi: 10.1109/TVT.2016.2555853.

[17] A. B. Dudekula and J. D. Naber, "Algorithm development for avoiding both moving and stationary obstacles in an unstructured high-speed autonomous vehicular application using a nonlinear model predictive controller," *SAE Int. J. Connected Automated Vehicles*, vol. 3, no. 3, pp. 161–191, Oct. 2020, doi: 10.4271/12-03-03-0014.

[18] B. Yang, X. W. Song, and Z. H. Gao, "Optimal obstacle avoidance trajectory planning algorithm considering vehicle motion constraints," *Automot. Eng.*, vol. 43, no. 4, pp. 562–570, 2021.

[19] F. Lin, K. Wang, Y. Zhao, and S. Wang, "Integrated avoid collision control of autonomous vehicle based on trajectory re-planning and V2V information interaction," *Sensors*, vol. 20, no. 4, p. 1079, Feb. 2020, doi: 10.3390/s20041079.

[20] Y. T. Tian, X. Y. Wang, L. L. Hu, Y. F. Lian, Y. Zhao, and C. Yin, "Active collision avoidance algorithm in electric vehicle lateral lane change," *J. Jilin Univ. Eng. Technol. Ed.*, vol. 46, no. 5, pp. 1587–1594, Sep. 2016, doi: 10.13229/j.cnki.jdxbgxb201605030.

[21] Q. Wu, W.-D. Liu, S.-Y. Guo, S. Cheng, S.-J. Li, H.-W. Liang, and Z.-J. Liu, "Research on lane-change strategy with real-time obstacle avoidance function," *IEEE Access*, vol. 8, pp. 211255–211268, 2020, doi: 10.1109/ACCESS.2020.3037103.

[22] L. Yuan, H. Zhao, H. Chen, and B. Ren, "Nonlinear MPC-based slip control for electric vehicles with vehicle safety constraints," *Mechatronics*, vol. 38, pp. 1–15, Sep. 2016, doi: 10.1016/j.mechatronics.2016.05.006.

[23] L. Zhai, C. Wang, Y. Hou, and C. Liu, "MPC-based integrated control of trajectory tracking and handling stability for intelligent driving vehicle driven by four hub motor," *IEEE Trans. Veh. Technol.*, vol. 71, no. 3, pp. 2668–2680, Mar. 2022, doi: 10.1109/TVT.2022.3140240.

[24] X. F. Pei, P. Li, Z. F. Chen, and X. X. Guo, "Research on active collision avoidance control of vehicles under different emergency conditions," *Automot. Eng.*, vol. 42, no. 12, pp. 1647–1654, Dec. 2020.

[25] H. Wu, M. X. Deng, J. Y. Zou, X. W. Xu, and Y. B. Yan, "Research on vehicle active collision avoidance control based on road adhesion coefficient estimation," *J. Wuhan Univ. Sci. Technol.*, vol. 45, no. 4, pp. 286–294, Aug. 2022, doi: 10.3969/j.issn.1674-3644.2022.04.007.

[26] Q. Cui, R. Ding, X. Wu, and B. Zhou, "A new strategy for rear-end collision avoidance via autonomous steering and differential braking in highway driving," *Vehicle Syst. Dyn.*, vol. 58, no. 6, pp. 955–986, Apr. 2019, doi: 10.1080/00423114.2019.1602732.

[27] S. L. Yuan and G. Zheng, "A warning model for vehicle collision on account of the reaction time of the driver," *J. Saf. Environ.*, vol. 21, no. 1, pp. 270–276, Oct. 2021, doi: 10.13637/j.issn.1009-6094.2019.0830.

[28] M. Brezak and I. Petrovic, "Real-time approximation of clothoids with bounded error for path planning applications," *IEEE Trans. Robot.*, vol. 30, no. 2, pp. 507–515, Apr. 2014, doi: 10.1109/TRO.2013.2283928.

[29] Y. Rasekhipour, A. Khajepour, S.-K. Chen, and B. Litkouhi, "A potential field-based model predictive path-planning controller for autonomous road vehicles," *IEEE Trans. Intell. Transp. Syst.*, vol. 18, no. 5, pp. 1255–1267, May 2017, doi: 10.1109/TITS.2016.2604240.

[30] P. E. Hart, N. J. Nilsson, and B. Raphael, "A formal basis for the heuristic determination of minimum cost paths," *IEEE Trans. Syst. Sci. Cybern.*, vol. SSC-4, no. 2, pp. 100–107, Jul. 1968, doi: 10.1109/TSSC.1968.300136.

[31] S. Karaman and E. Frazzoli, "Sampling-based algorithms for optimal motion planning," *Presented at 5th Rbobotics-Sci. Syst. (RSS) Conf.* Zaragoza, Spain: Univ Zaragoza, Jun. 2010, vol. 30, no. 8, pp. 846–894, doi: 10.1177/0278364911406761.

[32] J. Wang, W. Chi, C. Li, C. Wang, and M. Q.-H. Meng, "Neural RRT*: Learning-based optimal path planning," *IEEE Trans. Autom. Sci. Eng.*, vol. 17, no. 4, pp. 1748–1758, Oct. 2020, doi: 10.1109/TASE.2020.2976560.

[33] C. C. Yuan and Y. J. Sun, "Research on lane-changing collision avoidance system of intelligent vehicle based on extension control," *J. Chongqing Univ. Technol.*, vol. 34, no. 9, pp. 29–38, Sep. 2020.

[34] P. Falcone, F. Borrelli, J. Asgari, H. E. Tseng, and D. Hrovat, "Predictive active steering control for autonomous vehicle systems," *IEEE Trans. Control Syst. Technol.*, vol. 15, no. 3, pp. 566–580, May 2007, doi: 10.1109/TCST.2007.894653.

[35] C. F. Hu, L. Cao, L. X. Zhao, and N. Wang, "Model predictive control-based steering control of unmanned ground vehicle with tire blowout," *J. Tianjing Univ.*, vol. 52, no. 5, pp. 468–474, Jun. 2019, doi: 10.11784/tdxbz201809084.

SHENGQIN LI received the Ph.D. degree in transportation engineering from Northeast Forestry University, Heilongjiang, China, in 2008.

She is currently an Associate Professor with the School of Transportation, Northeast Forestry University. She has authored more than 30 journal articles. Her current research interests include vehicle system dynamics and control, vehicle active safety technology, intelligent vehicle handling, and stability control.

QINGQING ZHAO is currently pursuing the Ph.D. degree with Northeast Forestry University.

She has authored more than ten journal articles. Her current research interests include vehicle active safety technology, intelligent vehicle handling, and stability control.